

# Measurement of the Amount of Scale Formed in the Process of Heating the Steel Charge in Industrial Conditions

Jarosław Boryca<sup>1</sup>

<sup>1</sup>Department of Production Management, Faculty of Production Engineering and Materials Technology, Czestochowa University of Technology, 42-201 Czestochowa, Al. Armii Krajowej 19, Poland, e-mail: [jaroslaw.boryca@pcz.pl](mailto:jaroslaw.boryca@pcz.pl)

Category : Original Scientific Paper

Received : 21 June 2022 / Revised: 29 June 2022 / Accepted: 30 June 2022

*Keywords* : amount of scale, heating of steel charge, industrial measurements, scale,

*Abstract* : The article presents methods for determining the amount of mill scale formed in the process of heating the steel charge before plastic working. Relationships allowing to calculate the amount of scale, its thickness and loss of steel were presented. Measurements and calculations were made for the selected method. The results and conclusions are presented.

*Citation*: Boryca Jarosław: Measurement of the Amount of Scale Formed in the Process of Heating the Steel Charge in Industrial Conditions, *Advance in Thermal Processes and Energy Transformation*, Volume 5, No.2 (2022), p. 18-21, ISSN 2585-9102 <https://doi.org/10.54570/atpet>

## 1 Introduction

Scale is a product of an oxidation reaction that forms on the surface of a metal or alloy. As a result of the oxidation of metals, solid oxidation products are formed in a wide range of temperatures [1, 2].

The basic elements determining the structure and phase composition of scale include [1,3]:

- ✓ type of metal,
- ✓ composition and pressure of the oxidizing environment,
- ✓ temperature and duration of the oxidation reaction,
- ✓ the concentration of alloying elements in the metallic phase.

The scale formed during the heating of the steel to the plastic working temperature consists of three iron oxides. They occur in the scale in the form of three parallel layers in the order corresponding to the oxygen content [4-6].

External factors are related to the oxidizing environment, i.e. its composition, temperature, pressure, gas velocity and other parameters. The most important external factors affecting the oxidation of steel include [1, 3]:

- ✓ heating time,
- ✓ temperature of the working space of the furnace (temperature of the surface of the heated steel),
- ✓ composition of the gas atmosphere.

To the processes of heating charge oxidization of steel accompanies without absenting.

Hereupon the phenomena there is a scale the presence of which presents a substantial problem identically for the process of heating as well as more late plastic working processing. The process of oxidization draws the considerable losses of steel, negatively influences on firmness of heat and mill-rolling devices, worsens to the property of heating steel and also reduces intensity of process of heating. With a purpose lowering of heating consumption it is needed to aspire to limitation of amount of nascent dross through the selection of the proper of heating technology [7].

By an important question, in relation to quality of heating process, there is influence of scale layer of on the terms of flow warm inwardly of charge. A scale comparatively with steel has a considerably smallest value of conductivity coefficient, from what negatively can influence on intensity of heating and draw growth of heat consumption or reduce the values of final temperatures in the cut of charge [8].

The amount of scale can also be represented by the thickness of its layer or by the loss of steel to scale. The amount of scale can be expressed in mass units or referred to the surface or mass of the steel charge [9-12].

## 2 The amount of scale measurement method

The amount of scale in relation to the weight of the charge can be determined by measuring the thickness of the scale. The thickness of the scale layer is determined by the following relationship:

$$\delta_{zg} = \frac{z}{\rho_{zg} \cdot \bar{X}_{Fe}}, \text{ m} \quad (1)$$

where:

$\rho_{zg}$  – scale density (3900 kg/m<sup>3</sup>),

$\bar{X}_{Fe}$  – average mass fraction of iron in scale

( $\bar{X}_{Fe} = 0.74$ ),

$z$  – surface loss of steel to scale, (kg/m<sup>2</sup>).

Thus, knowing the thickness of the scale layer, the steel loss can be determined:

$$z = \delta_{zg} \cdot \rho_{zg} \cdot \bar{X}_{Fe}, \text{ kg/m}^2 \quad (2)$$

The amount of scale formed during the heating of one billet can be determined from the relationship:

$$z' = \frac{z}{\bar{X}_{Fe}} \cdot A_w, \text{ kg} \quad (3)$$

where:

$A_w$  – outer surface of charge (billet), m<sup>2</sup>.

$$A_w = 2 \cdot b \cdot h + 2 \cdot b \cdot l + 2 \cdot h \cdot l, \text{ m}^2 \quad (4)$$

where:

$b, h, l$  – steel billet dimensions, m.

Volume billet:

$$V_w = b \cdot h \cdot l, \text{ m}^3 \quad (5)$$

The dimensions of the billet are shown in Fig. 1.

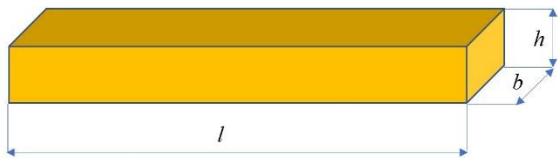


Figure 1 Dimensions of the billet

The mass of the billet will be:

$$m_w = V_w \cdot \rho_w, \text{ kg} \quad (6)$$

The amount of scale in relation to the charge mass will be:

$$z_{zg}'' = \frac{z'}{m_w}, \text{ kg}_{zg}/\text{kg}_w \quad (7)$$

In order to be able to use the first method, a sample of scale should be taken from the charge coming out of the furnace and its thickness measured with a micrometer. This method is less secure and less accurate.

The second method of determining the amount of scale consists in measuring the weight of the sample at individual stages of heating. The masses of the

samples before heating, after heating and after descaling must be determined, and the sample must pass through the furnace with the charge. The sample is cut from the billet coming out of the continuous steel casting process, i.e. the material that will be heated in the furnace (Figure 2).

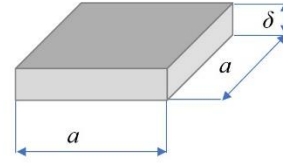


Figure 2 Dimension of steel sample

The amount of scale formed during the heating of one billet can also be determined from the relationship [12]:

$$z' = \frac{m_1 - m_2}{1000 \cdot A_p}, \text{ kg/m}^2 \quad (8)$$

where:

$m_1$  – sample mass after heating, g,

$m_2$  – sample mass after complete descaling, g,

$z'$  – amount of scale, kg/m<sup>2</sup>,

$A_p$  – surface of sample, m<sup>2</sup>.

$$A_p = 2 \cdot a^2 + 4 \cdot a \cdot \delta, \text{ m}^2 \quad (9)$$

where:

$a$  – side dimension of the sample, m,

$\delta$  – sample thickness, m.

The loss of steel to scale is determined according to the following relationship:

$$z = \frac{m_0 - m_2}{1000 \cdot A_p}, \text{ kg/m}^2 \quad (10)$$

where:

$m_0$  – sample mass before heating, g.

Further calculations are carried out in accordance with the previous procedure using dependencies (1), (3) and (7).

In order for the sample to pass through the furnace, it must first be placed in a special rack (Figure 3) and then fixed on the billet (Figure 4) [12].

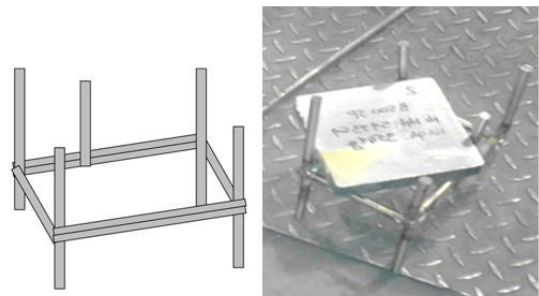


Figure 3 View of the special rack and rack with the sample



Figure 4 View of a sample and rack applied to a billet placed in a heating furnace

### 3 Measurement and calculation results

Measurements and calculations were made using the second method of determining the amount of scale.

After removal from the furnace, the samples were cooled down and then weighed. Figure 5 shows a cooled sample subjected to the mass measurement process.



Figure 5 View of a cooled sample subjected to weighing

Mass measurements were repeated after complete descaling of the sample (Figure 6).



Figure 6 View of a sample after complete descaling subjected to weighing

The results of mass measurements for selected cases are presented in Table 1. The results of scale

calculations are presented in Table 2. The following surfaces were taken into account in the calculations:

- cold charge  $A_p = 0.06144 \text{ m}^2$ ,
- warm charge  $A_p = 0.06336 \text{ m}^2$ ,
- hot charge  $A_p = 0.06464 \text{ m}^2$ .

Table 1 The results of mass measurements for different charge temperatures at the entrance to the furnace

	cold charge (20°C)	warm charge (350°C)	hot charge (700°C)
$m_0, \text{ g}$	3281	3832	4059
$m_1, \text{ g}$	3349	3898	4123
$m_2, \text{ g}$	3153	3716	3965

Table 2 The results of amount scale calculations for different charge temperatures at the entrance to the furnace

	cold charge (20°C)	warm charge (350°C)	hot charge (700°C)
$z', \text{ kg}\cdot\text{m}^{-2}$	3.1901	2.8725	2.4443
$z, \text{ kg}\cdot\text{m}^{-2}$	2.0833	1.8308	1.4542
$\delta_{zg}, \text{ mm}$	0.7219	0.6344	0.5039
$z''_{zg}, \text{ kg}_{zg}\cdot\text{t}_w^{-1}$	0.0527	0.0409	0.0313

### 4 Conclusions

The problem of scale formation is important for many reasons. Too much scale causes an increase in fuel consumption in heating furnaces, hence it is so important to reduce the amount of scale.

The presented methods make it possible to determine the amount of scale in various forms (also as a loss of steel or the thickness of the scale layer). More accurate and less dangerous is the second method, using a special stand placed on the heated billet.

The results of the measurements and calculations carried out indicate the correctness of the methodology. The amount of scale determined during industrial tests corresponds to theoretical studies and experimental tests.

## The reference list

- [1] MROWEC, S.: *Kinetyka i mechanizm utleniania metali*, Katowice, Śląsk, 1982.
- [2] FROMHOLD, A.T.: *Theory of Metal Oxidation*, Amsterdam, North-Holland, 1976.
- [3] BORYCA, J.: Ph.D. Thesis *Przyczepność warstwy zgorzeliny powstałej w procesie nagrzewania wsadu stalowego*, Politechnika Częstochowska, Częstochowa 2005.
- [4] BALA, H.: *Korozja materiałów – teoria i praktyka*, Prace dydaktyczne Wydziału Inżynierii Procesowej, Materiałowej i Fizyki Stosowanej, Seria Inżynieria Materiałowa nr 5, Częstochowa 2002.
- [5] KIELOCH, M.: *Technologia i zasady nagrzewania wsadu*, Skrypt Politechniki Częstochowskiej, Częstochowa 1995.
- [6] BAE-KYUN, K, SZPUNAR, J.A.: Orientation imaging microscopy for the study on high temperature oxidation, *Scripta Materialia*, Vol. 44, No. 11, pp. 2605-2610, 2001.
- [7] PIECHOWICZ, Ł.: Ph.D. Thesis *Zużycie ciepła a straty stali w procesie nagrzewania wsadu*, Politechnika Częstochowska, Częstochowa 2008.
- [8] BORYCA, J., KIELOCH, M., PIECHOWICZ, Ł.: Modeling of the Influence of Technology and Productivity on Thickness of Scale Layer in the Heating Steel Charge Process, *Acta Metallurgica Slovaca*, Vol. 15, No.1, pp. 37 – 43, 2009.
- [9] BORYCA, J., WYLECIAŁ, T.: Calculation of Measurement Errors in Research of Adhesion of Scale to the Steel Substrates for Cold Specimens, *Advances in Thermal Processes and Energy Transformation*, Vol. 2, No. 4, pp. 61 – 64, 2019.
- [10] BORYCA, J., WYLECIAŁ, T., URBANIAK, D.: Measurement Errors in Research of Adhesion of Scale to the Steel Substrates, *Advances in Thermal Processes and Energy Transformation*, Vol. 1, No. 1, pp. 5 – 9, 2018.
- [11] BORYCA, J., KOLMASIAK, C., WYLECIAŁ, T., URBANIAK, D., OTWINOWSKI, H.: Experimental Measurements of Scale Adhesion for a Pre-Oxidized Steel Charge, *Metalurgija*, Vol. 6, No.3-4, pp. 368 – 370, 2021.
- [12] BORYCA, J., WYLECIAŁ, T., URBANIAK, D.: Influence of Initial Charge Temperature and Furnace Exploitation on Steel Loss, *Archives of Metallurgy and Materials*, Vol. 67, No. 1, pp. 289 – 291, 2022.

# Laminar Air Curtains as Protection against Respiratory Infections

Vladislav Chovanec<sup>1</sup> • Lucia Bursíková<sup>1</sup>

*<sup>1</sup>Institute of Energy Machinery, Slovak Technical University, Faculty of Mechanical Engineering, Námetie slobody 17, 812 31 Bratislava, Slovak Republic, [vladislav.chovanec@stuba.sk](mailto:vladislav.chovanec@stuba.sk), [lucia.bursikova@stuba.sk](mailto:lucia.bursikova@stuba.sk)*

Category : Original Scientific Paper

Received : 11 June 2022 / Revised: 24 June 2022 / Accepted: 28 June 2022

Keywords : air curtain, air chamber, CFD simulation, design optimization

*Abstract : The article focuses on the design, optimization and implementation of a device for creating a laminar air curtain. Its purpose is to separate two spaces filled with air of different parameters, while these air masses do not mix. The function of the device is to prevent the transmission of respiratory pathogens that can be transmitted through the air. The premises can also be disinfected with a volatile inhalant. In the experimental device, air flow speeds are measured in two parts, namely in the part at the entrance of the air curtain to the chamber and in the part at the exit from it. Based on these measurements, velocity profiles are compiled, which are compared with verified simulations of the experimental device in CFD. The results indicate whether the device needs to be optimized, especially with regard to a more suitable geometry of the outlet and the laminar chamber. The new design is verified again in CFD simulation and finally implemented, so that it meets the requirements arising from the purpose of the device and is additionally verified by new measurements.*

*Citation: Chovanec Vladislav, Bursíková Lucia: Luminar Air Curtains as Protection against Respiratory Infections, Advance in Thermal Processes and Energy Transformation, Volume 5, No. 2, (2022), p. 22-29, ISSN 2585-9102. <https://doi.org/10.54570/atpet>*

## 1 Introduction

If we look at devices that are used in the world and are similar to ours, they are mostly air curtains capable of separating the air of two spaces, for example, a cold and a warmer part, such as the exterior and interior of a building. The design is usually in the form of an air curtain. However, this system can also separate spaces filled with air of different quality and composition. An example can be a situation where there are a lot of people coming and going during the day, such as clients, and on the other hand, a counter worker is present for several hours. The protection of the worker could consist in the use of an air curtain and the division of the space into two parts, both separately ventilated. The purpose of the device is to prevent the spread of disease-causing and infectious germs and viruses by stopping the mixing of two air masses of different quality. It would thus be possible to protect persons in these separate spaces from the risk of infection. The quality of air particles separated by an air curtain can also be continuously modified by inhalant substances. Possibilities of application are, for example, at the post

office, in shops or schools, or in public and suburban transport vehicles.

Another goal during the development is to maintain the simplicity of the construction, reasonably low price and easy installation of the system, so that the system can be deployed quickly and efficiently in the event of an impending or outbreak of an epidemic. It is also taken into account that the device can be built in the designated location mostly from available resources and parts. For this reason, during the construction of the system, a maximum of the existing air-conditioning parts (fans, pipes, outlets, nozzles) are used, which were purchased, and special attention is paid only to critical components [1,2].

## 2 Existing air air conditioning solutions and devices

In industry and in the residential sphere, there are many air-conditioning devices whose purpose is to separate two air masses with different parameters. Some of them are used in our experimental device and meet the

function and purpose. I will list some of the most important air conditioning equipment.

### 2.1 Air curtains

They are air-conditioning devices that separate two environments using an optically non-disturbing air flow. They are mainly used in buildings and shops. There is frequent opening and closing of the front door. Components such as fans, nozzles, pipes and others are used in air curtains. Air outlets are a functional part of ventilation and air conditioning equipment. They finish the ventilation air duct networks, and the correct function of the entire system depends on their design, dimensioning and actual execution. Outlets for air supply to the space have a decisive influence on spatial flow, temperature fields and the concentration of harmful substances and impurities.

Types of outlets:

- Blinds (classic outlets)
- Anemostats
- Nozzles with swirling effect
- Slots-slit outlet

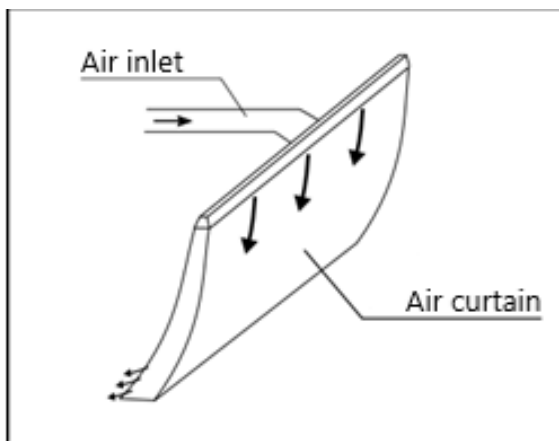


Figure 1 The principle of the outlet function [2]

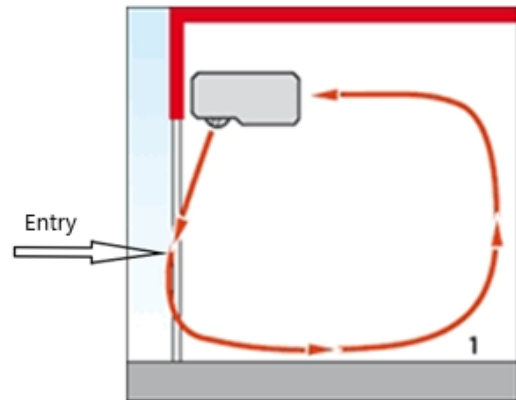


Figure 2 The air curtain above the entry [2]

### 2.2 Laval nozzle

In our experiment, it is possible to use the created model of the nozzle, which although has a base in a slotted nozzle, but its cross-section has the shape of a Laval nozzle. In practice, it serves to convert the pressure drop into the kinetic energy of the gas during its expansion.

### 3 Basic design

In the basic design, we started from the effort to separate two spaces in which people find themselves with an air curtain - a wall so that they are still able to communicate verbally and remain in visual contact. The essence of the technology for creating such a wall is the equipment used in air curtains. It is advisable to design and use a laminar chamber in which air filtering can be applied directly. The design will also take into account the speed of exhaled air of two people sitting or standing opposite each other. At the same time, this experimental device will be the carrier of all the functional elements that are necessary to carry out the experiments. It is also important to ensure that the functional elements can be launched from one place for more convenient handling and control, and last but not least, that it is possible to modify and add additional elements or carriers relatively easily, so that it does not affect the main function of this experimental device. The initial mathematical model was created with the simplest possible construction in the Solid Works program. The first CFD simulations were based on this mathematical model.

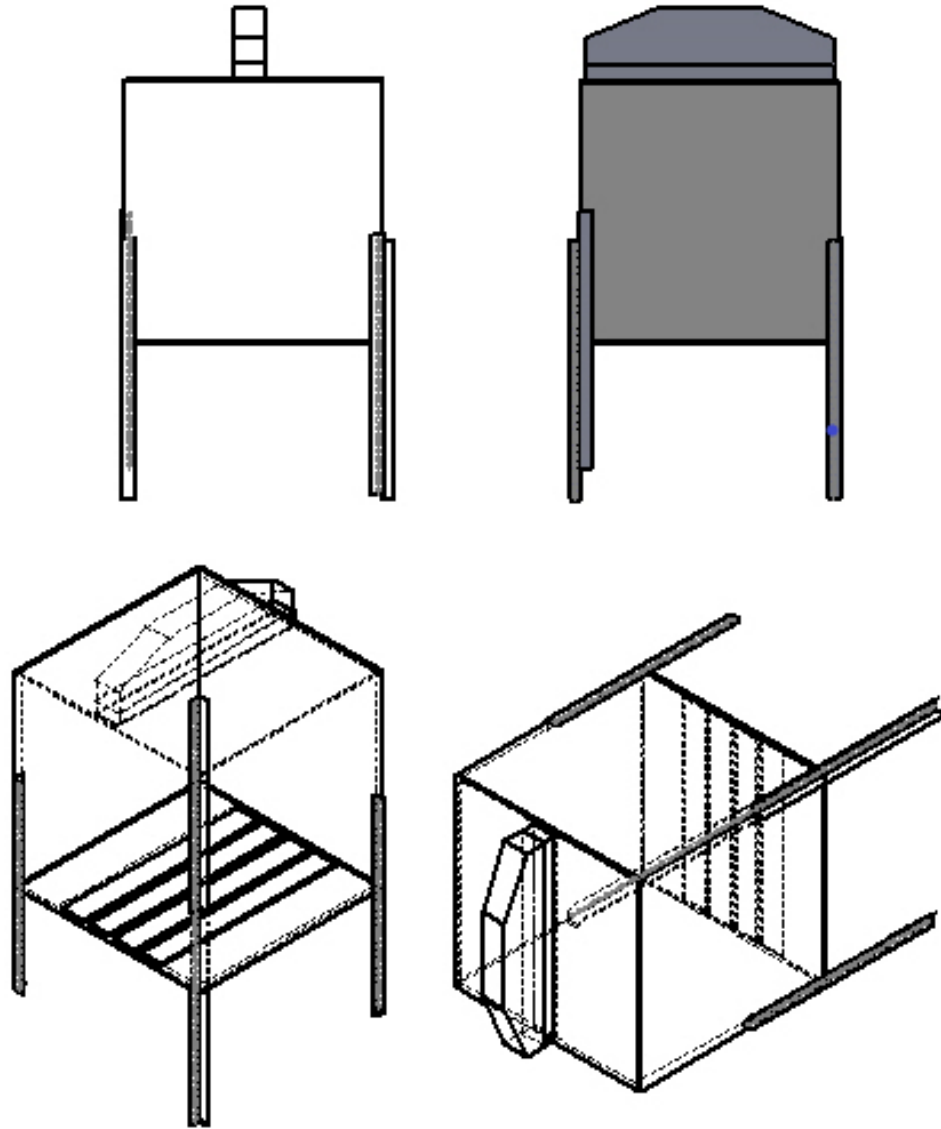


Figure 3 Basic geometric model - preliminary design in the Solid works program

#### 4 CFD simulations - geometry, network and settings

First, we defined the geometry of our experimental setup. It was created in the Design Modeler program, which is part of Ansys Workbench. For this geometry, we have created a calculation network 'Mesh', on which the calculation should take place. Next steps has been focused on CFD simulation using the Ansys Fluent program. The result was the model in the following figure, which was used for initial simulations with different input parameters.

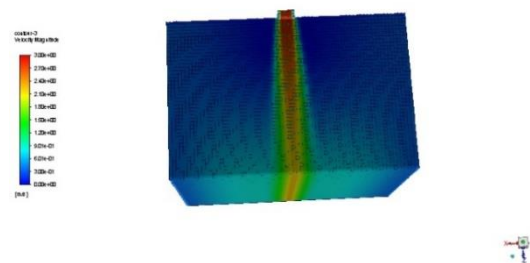


Figure 4 Optimized basic model of the device built in the laboratory from available purchased parts

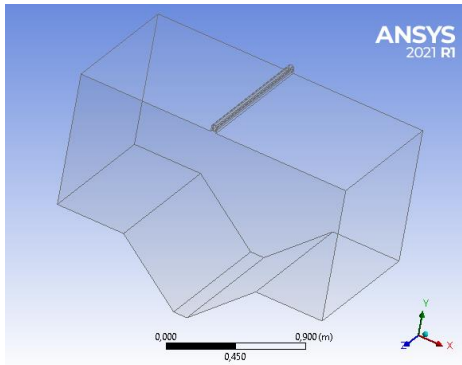


Figure 5 Initial design of the experimental device

In the picture, it is possible to see significant turbulence that extends almost to the people sitting opposite. In the first design, air extraction in the lower part of the device in a narrow place was not considered, only a free outlet. Due to the turbulence. There was modification of some parameters and the device so that the lower part partially directs the possible turbulence and so it does not spread further to the sides. For this reason, it is possible to open the bottom of the device up to an angle of  $90^\circ$ , if necessary to change the angle of the flow of the air curtain or create larger area for suction. With this in mind, we adjusted the geometry and added a positionable triangular outlet space, a covered recess in the bottom, at the end of which there is an opening for air suction. This model turned out to be less turbulent in the simulations and the flow was better directed.

## 5 Design, implementation and test results

Based on the results of optimization simulations and model modifications, the realization of the physical model began. The device has four main parts:

1. An internal space in which air flows by natural or forced convection.
2. Lower space in the shape of a triangular prism that can be changed to a cuboid, space for suction.
3. Upper space with a carrier for devices such as a nozzle and fan with pipe.
4. Side compartment with control panel box and regulators, including storage of fans and pipes.

The following pictures show the construction of the experimental device:



Figure 6 Built experimental device

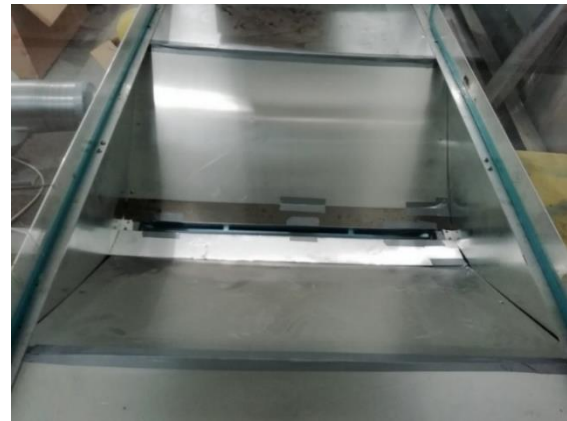


Figure 7 Internal space-suction recess



Figure 8 Bottom space for suction

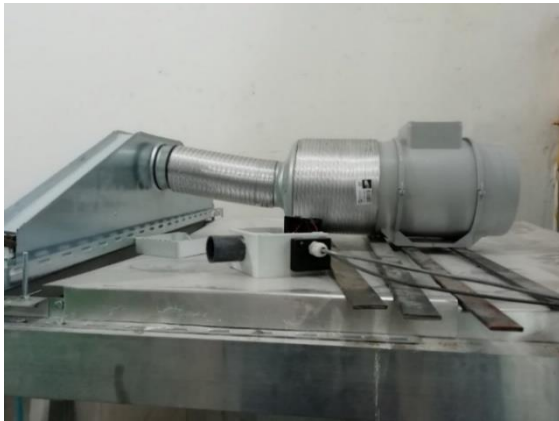


Figure 9 Upper space - system forming an air curtain

## 6 Measurements and results of measurements during experiments - findings

### 6.1 Smoke test

In initial tests, there was performed a smoke test to verify the veracity of the simulation and the suitability of device and parts geometry. Thanks to the smoke from the smoke machine, which is discharged at a certain speed and direction, it is possible to realistically visualize the air flow and more quickly to find the places of turbulence. The principle of the smoke machine's function is the use of a special liquid, which is glycerol or glycol dissolved in distilled water, and it is pumped into hot copper tubes, the end of which is fitted with a nozzle [11].

### 6.2 Description of the smoke test process

The smoke machine was placed in front of the experimental device and turned with the smoke discharge nozzle towards the device. The smoke was dosed in small volumes and at different time intervals in such a way that it was possible to capture the behavior of the smoke in contact with the air curtain. The speed of the air curtain was not evenly distributed, it differed in different parts of the outlet exit. Based on the smoke test, it was also verified that the draft in the lower part of the experimental device is not sufficient or laminar when using the available parts in the laboratory according to the initial design. It will therefore be necessary to adjust the geometry of the suction device, or to test the laminarity of the curtain when using an overflow into the space under the device. Next, we measured the velocity profiles at the exit from the outlet and at the entrance to the suction chamber with an anemometer. From the measurements we found that the velocities are very different and the measurement confirmed the findings from the smoke test, I then verified this finding with the CFD model. The results of velocity measurements are visualised below.

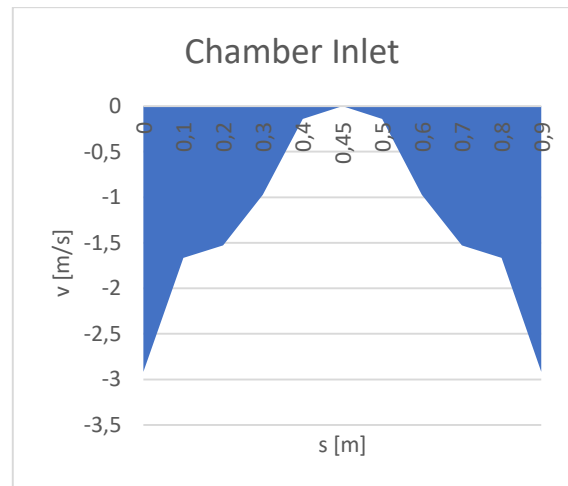


Figure 10 Measured velocity profile of the curtain at the entrance along the outlet

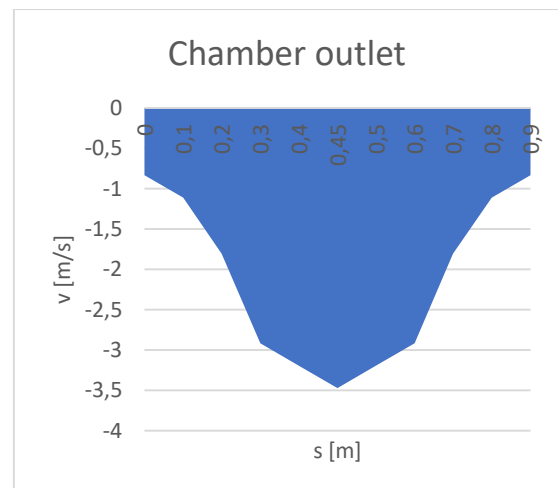


Figure 11 Measured velocity profile of the curtain at the exit to the chamber along the outlet

### 6.3 Comparison of measured values by CFD simulation

In order to compare the results from the smoke test and the measurement of velocities with an anemometer, we created a simulation of the experimental device in its current state, where a laminar chamber with a slot outlet was used [12-17].

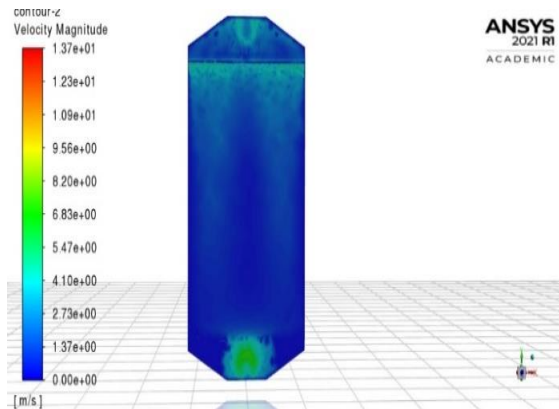


Figure 12 Velocity profile of curtains with the flow connection box at a speed of 4 m/s from the fan

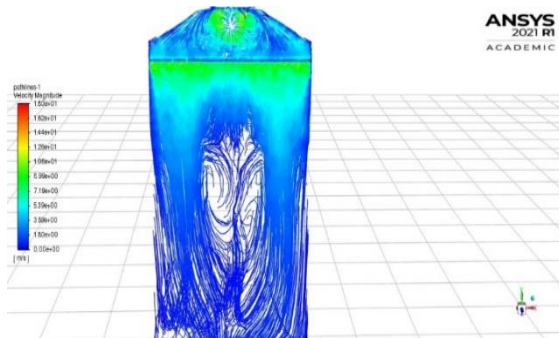


Figure 13 Speed profile of the screen with the flow connection box and outlet at a speed of 7 m/s from the fan

## 7 Options for further progress and optimization of the device based on tests

From the results of previous measurements and tests, it follows that the device needs to be adjusted so that it fulfills the required function.

The options for the next procedure and solution are:

1. Creation of a laminar chamber at the inlet from ventilator V1.
2. Creation of a laminar chamber and use of another outlet nozzle of a more suitable shape.
3. Omitting the outlet nozzle using a laminar chamber and leaving the outlet free.
4. Creating a laminar chamber and directing the flow with suitable vanes.
5. Use of a system of nozzles connected to the compressor, which will be installed on the ceiling.

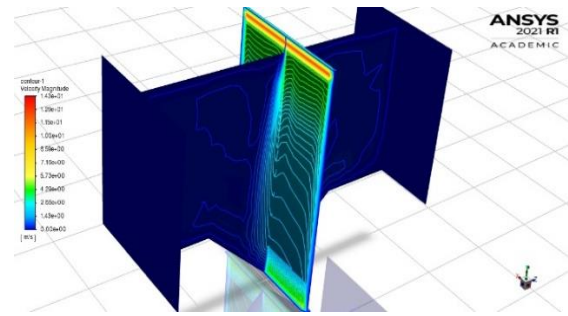


Figure 14 Velocity profile of curtain using a nozzle with a nozzle geometry

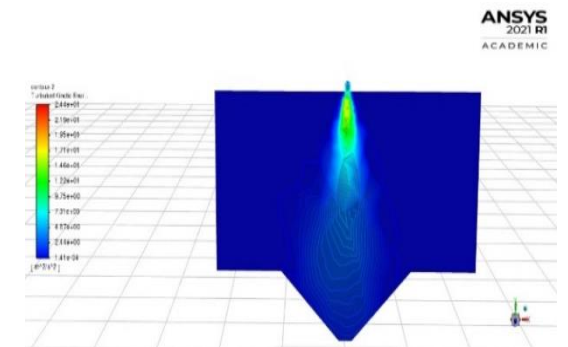


Figure 15 Velocity profile using suitable modified vanes and laminar chamber

## 8 Discussion

The current state of the device is at the level of modifications of model geometry of the laminar chamber and outlet and simulation testing. Based on the outputs, a prototype of a laminar chamber and an outlet of suitable shape will be built. The geometry of the model is created on the basis of calculations and simulations based on them, which were based on the volume flow graph at a given pressure and the fan data table. The pressure losses on the pipeline and in the laminar chamber were also calculated. Graph was created from which we determine the working point of the fan. Following relations were used to calculate both local and length losses:

$$\lambda = \xi \cdot \frac{L}{d} \quad (1)$$

$\xi$  coefficient of local losses [-]

$\lambda$  coefficient of length losses [-]

L length [m]

D diameter [m]

and for local losses:

$$p_{zt} = \frac{\lambda}{d} \cdot \rho \cdot \frac{w^2}{2} \cdot l \quad [\text{Pa}] \quad (2)$$

For a square pipe, we use the relation to calculate the equivalent diameter:

$$d_{ekv} = \frac{2 \cdot A \cdot B}{A + B} \quad [\text{m}] \quad (3)$$

where A and B are the width and height of the pipe [m]

and

$$Z = \xi \cdot \frac{v^2}{2g} \quad [\text{Pa}] \quad (4)$$

The design of the built device is complex, consisting of several functional and structural elements connected to each other. The electricity consumption in our project is 265 W at maximum fan rotation. The physical part of the model according to the simulations was made in the large laboratory of the Institute of Energy in the Heavy Laboratory of the Sjf STU due to the possible additional space needed for measurements and research and also for easier handling during the construction and delivery of additional equipment, positioning of fans and also the necessary space for better dispersal of air leaving device.

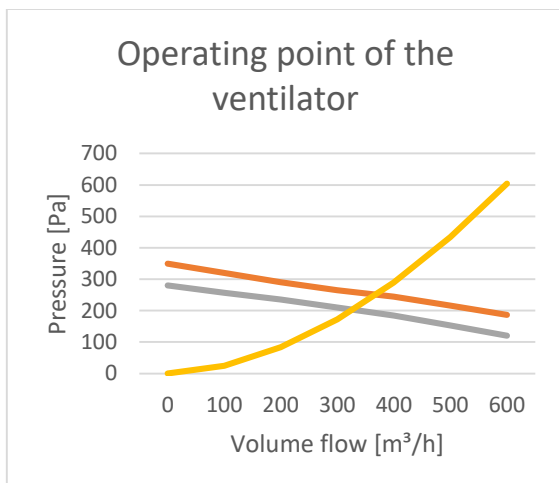


Figure 16 Characteristics of the fan and working point

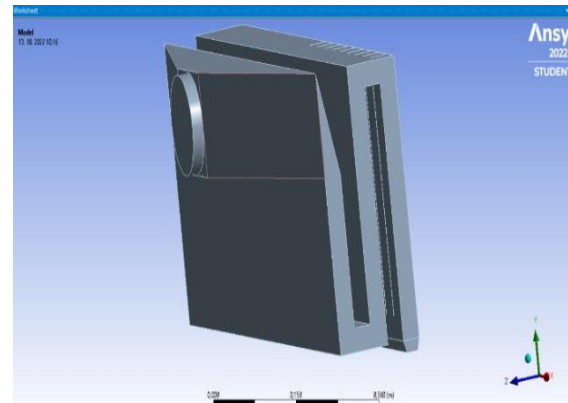


Figure 17 Laminar chamber geometry, current design

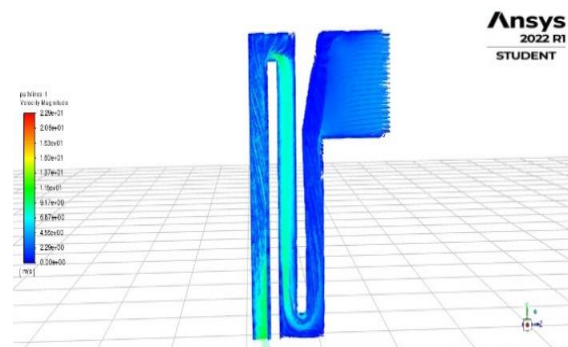


Figure 18 Laminar chamber geometry, air flow through it

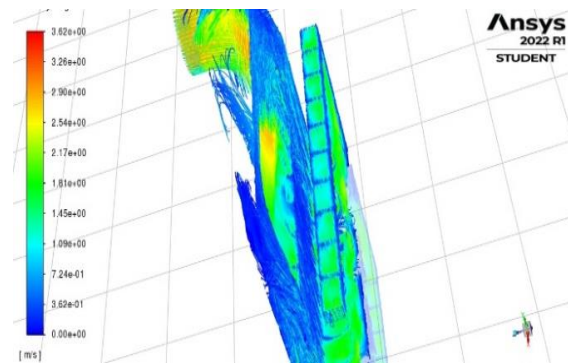


Figure 19 Velocity profile in a laminar chamber using dividing baffles

## 9 Conclusion

The article analyzes the use of air as a separating medium by creating an air curtain with possible modification of properties and composition. The focus of this project is the direction of the air entering by forced convection from the laminar flow fan in the form of an air curtain. It separates two spaces containing air masses of different quality. To achieve this, we will use devices such as a nozzle and a laminar chamber connected to it, using paddles to direct the flow, or using a air outlets in the shape of a nozzle or a or a nozzle system. The main task is not to let pass microbiological particles such as viruses in air or water droplets and dirt from one space to another. Reasonable price, reliability, easy maintenance and simple construction are also

important requirements. It will be mainly used in public places where one person comes into constant contact with a lot of people, such as school teachers, public transport drivers and intercity drivers, as well as counter workers in banks, post offices and so. The experimental device is still in the modification and testing phase.

#### The reference list

- [1] SZÉKYOVÁ, M., FERSTL, K., NOVÝ, R.: *Vetranie a klimatizácia*, Jaga group, 2004.
- [2] MASARYK, M.: *Antiinfekčná ochrana vzduchovými bublinami a stenami*, (2019).
- [3] Potrubní ventilátor Dalap. [Online], Available: <https://www.vzduchotechnika-ventilatory.cz/potrubni-ventilator-dalap-vpi-200-axialni/> [24 May 2022], 2022.
- [4] Regulátory otáčok a prepínače rýchlosti. [Online], Available: <https://www.firn.sk/rs-5-0-t-p2477> [20 May 2022], 2022.
- [5] BRAUN, G.-J., ZEILER, W.: CO<sub>2</sub>-concentration of the surrounding air of sleeping infants inside a crib, *International Journal of Ventilation*, Vol. 20, No. 3-4, pp.161-171, 2020.
- [6] HEINZ, P.: ADJOINT SOLVER, Bachelor's thesis, Brno University of Technology, Energy Institute, Faculty of Mechanical Engineering, Brno, 2018.
- [7] KOČÍK, M.: Dýmstroj. [Online], Available: <http://zavodsky1.szm.com/schemy/ostatne/dymstroj.htm> [20 May 2022], 2022.
- [8] Ejectors. Managed by CanmetENERGY at the Varennes (Quebec) research centre. [Online], Available: [https://www.nrcan.gc.ca/sites/www.nrcan.gc.ca/files/canmetenergy/files/2009-185\\_e.pdf](https://www.nrcan.gc.ca/sites/www.nrcan.gc.ca/files/canmetenergy/files/2009-185_e.pdf) [20 May 2022], 2022.
- [9] Vzduchové clony. [Online], Available: <https://shop.systemair.com/sk-SK/vzduchove-clony/c38731> [18 May 2022], 2022.
- [10] ŠKORPÍK, J.: Proudění par a tekutin. Lavalova tryska. [Online], Available: <https://www.transformacni-technologie.cz/40.html#lavalova-tryska-konvergentne-divergentni-tryska> [20 May 2022], 2022.
- [11] MLKVIK, M., JEDELSKÝ, J., KARBSTEIN, H.P., GAUKEL, V.: Spraying of Viscous Liquids: Influence of Fluid-Mixing Mechanism on the Performance of Internal-Mixing Twin-Fluid Atomizers, *Appl. Sci.*, Vol. 10, No.15, 5249, 2020.
- [12] KNÍŽAT, B., HLBOČAN, P., MLKVIK, M.: CFD simulation of a natural circulation helium loop. *Scientific proceedings 2014*, Faculty of Mechanical Engineering, STU in Bratislava, 2014.
- [13] YANG, L., YE, M., HE, B.-J.: CFD simulation research on residential indoor air quality, *Sci. Total Environ.*, Vol.472, pp. 1137-1144, 2014.
- [14] VILLAFRUELA, J.M., OLMEDO, I., RUIZ DE ADANA, M., MÉNDEZ, C., NIELSEN, P.V.: CFD analysis of the human exhalation flow using different boundary conditions and ventilation strategies, *Building and Environment*, Vol.62, pp. 191-200, 2013.
- [15] AGANOVIČ, A., STEFFENSEN, M., CAO, G.: CFD study of the air distribution and occupant draught sensation in a patient ward equipped with protected zone ventilation, *Building and Environment*, Vol. 162, 106279, 2019.
- [16] VILÁGI, F., KNÍŽAT, B., MLKVIK, M., URBAN, F., OLŠIAK, R., MLYNÁR, P.: Mathematical model of steady flow in a helium loop, *Mechanics & Industry*, Vol. 20, p.704, 2019.
- [17] ŠTRBA, D.: *Solárne ejektorové klimatizačné systémy*, Dissertation thesis, SjF STU Bratislava, 2021.

#### Acknowledgement

This article was supported by the state grant agency – project APVV 21-Development and experimental verification of a climate-adaptive transparent facade with multi-stage use of renewable energy sources for low-exergy radiant systems.

# Analysis of Wastewater Heat Recovery Potential for a Family House in Slovakia

Adam Miča<sup>1</sup> • Andrej Kapjor<sup>2</sup>

<sup>1</sup>Department of Power Engineering, Faculty of Mechanical Engineering, University of Žilina, Veľký diel, 010 26 Žilina, Slovakia, [adam.mica@fstroj.uniza.sk](mailto:adam.mica@fstroj.uniza.sk)

<sup>2</sup>Department of Power Engineering, Faculty of Mechanical Engineering, University of Žilina, Slovakia, [andrej.kapjor@fstroj.uniza.sk](mailto:andrej.kapjor@fstroj.uniza.sk)

Category : Original Scientific Paper

Received : 10 June 2022 / Revised: 22 June 2022 / Accepted: 24 June 2022

Keywords : heat pum , heat recovery, wastewater, water consumption

**Abstract:** All of us have begun to notice the effects of global warming and climate change. Moreover, the current trend in energy prices has reached a point where the concept of energy poverty is becoming more and more prevalent in society. If we want to change this situation, we need to approach energy and work with it very responsibly. That is why heat recovery within households is a key factor in improving the energy economy. Heat recovery from the exhaust air is more or less mandatory for new family houses in Slovakia. The energy contained in wastewater is essentially unused in Slovakia. In this study, we have performed an analysis of the potential of the energy contained in wastewater for a 4-member household of a family house.

**Citation:** Miča Adam, Kapjor Andrej: Analysis of Wastewater Heat Recovery Potential for a Family House in Slovakia, *Advance in Thermal Processes and Energy Transformation*, Volume 5, No.2, (2022), p. 30-35, ISSN 2585-9102. <https://doi.org/10.54570/atpet>

## 1 Introduction

The goal of the European Union is to achieve a neutral carbon footprint, so it is necessary to deal with effective technologies that will help us reduce the impact on the environment. The goal of the Paris Agreement is to keep the increase in global temperature well below 2°C and strive to keep it at 1.5°C [1]. The Slovak Republic had a share of energy from renewable sources in gross final energy consumption in 2020 of 17.3% [2]. Due to the set goals of the European Union, the use of renewable resources has become very interesting in recent years. In its investment plan [1], the European Union has set aside funds to support projects dealing with heat recovery. At the same time, in the legislative directive, the EU included wastewater in the category "energy from the environment", which is defined as a renewable energy source under certain conditions [3].

## 2 Usage of Heat From Wastewater

There are several ways in which we can obtain heat from wastewater. In the professional community, it was customary to divide individual methods into four basic levels at which wastewater heat recovery

(WWHR) can work: the Component level, Building level, Sewer level, and Wastewater treatment plant.

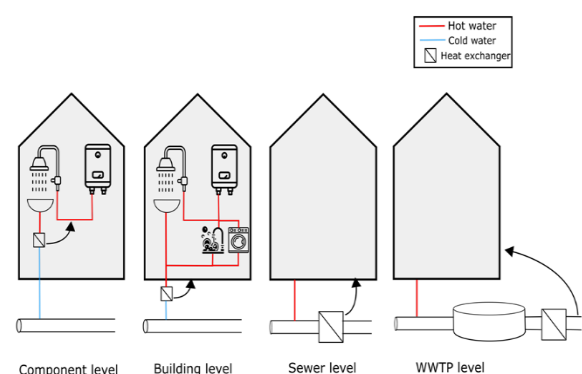


Figure 1 Potential wastewater heat recovery sites [4]

At the building level, the recovery of heat from the joint discharge of wastewater from one whole building is considered. The wastewater flow rate and temperature characteristics of this discharge depend on the type of building. Wastewater in apartment buildings can maintain a temperature of 10–25°C throughout the year. At this level, to perform heat recovery, wastewater is normally collected in a holding

tank and heat is recovered using a heat exchanger or water source heat pump. A grease capture system is usually used to prevent fouling and capture impurities in the wastewater. The general schematic diagram of WWHR with a heat pump is shown in Figure 1 [4].

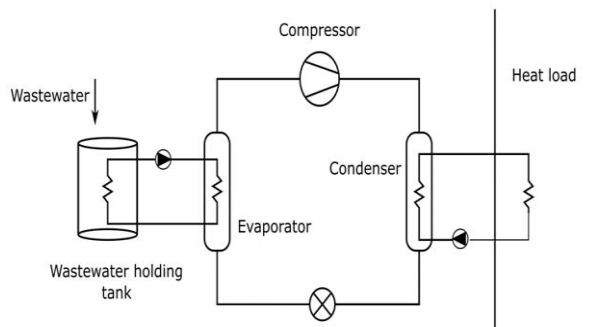


Figure 2 Wastewater heat recovery scheme at the building level with heat pump [4]

## 2.1 Concept of design

Our concept is designed for a family house with 4 people. We will put a collector in a 21 m<sup>3</sup> waste water tank, which will transport the unused energy from the wastewater to the evaporator of the heat pump. The 4 kW evaporator will increase the quality of the energy from the collector so that we can use it for DHW heating. If the collector does not have the necessary power, the outdoor unit of the heat pump will be triggered to compensate for the power difference (required for DHW and collector power) so that we can maintain the temperature of the water in the DHW tank in the range of 50 to 60°C.

## 3 Wastewater consumption model

The first step in heat recovery is to identify the potential of the heat source. Detailed information on the temperature of wastewater does not appear in the literature. Several types of research have been carried out in the world in recent years, the aim of which was to obtain the necessary information about the temperature and flow of wastewater. Cipolla and Maglionico [5] monitored the temperature and flow in the sewers in the city of Bologna. According to their measurements, the temperature never dropped below 11°C. They also came up with a similar measurement result as Ceconet et al. [6], which applied technologies for heat recovery from sewage to a multifunctional building in the center of Brno. In Sweden, the wastewater temperature at the object level is approximately 20 °C, and 8 to 12°C is reported in the sewage system after heat transfer to the environment (ground) [7]. However, several studies and experimental installations agree on the wastewater temperature range of 10 to 25°C [4, 8].

The main parameter in the system will be the consumption and temperature of water in the home. The information portal of the department of the Ministry of the Environment of the Slovak Republic states that in 2015 the specific need for drinking water supplied to households under the administration of Water Companies reached a value of 77,3 l.per<sup>-1</sup>.day<sup>-1</sup> [9].

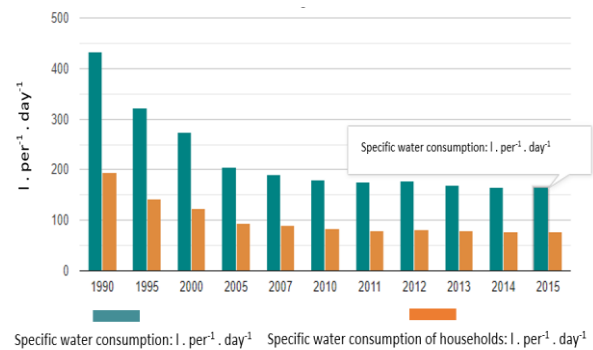


Figure 3 Specific water consumption per person [9]

Our model of water consumption was based on a study conducted by Wärrff [10], where they state a daily water consumption of 184 l per person, and at the same time, we also took into account the data provided by the Ministry of the Environment (see Figure 3 Specific water consumption per person), where water consumption per person was 169 l per day. We have defined 175 l per person per day as a reference value for total water consumption. To determine the mean temperature of the wastewater, we were based on research conducted by [8], where their measurements of hot water (see Figure 5) show that the approximate average value of hot water is 50°C and the average temperature of cold water is 19°C. According to measurements by the Swedish Energy Agency, 55 l of hot water represents approximately 30 % of the total water consumption of 184 l [8]. We set as reference ratio 30 % of hot water and 70 % of cold water of the total water consumption. The temperature of the hot water range from 50 to 60°C depending on the DHW tank. The temperature of the cold water was 10°C.

The daily water consumption model was based on the similarity in the graph of water consumption at the Swedish Energy Agency [10] and the measurements made in the work [8]. Where you can see the increased consumption in the morning hours approximately in the interval from 5:00 a.m. to 10:00 a.m. Subsequently, water consumption during the day decreases until 17:00, when water consumption increases again to approximately 50 % compared to the morning peak consumption.

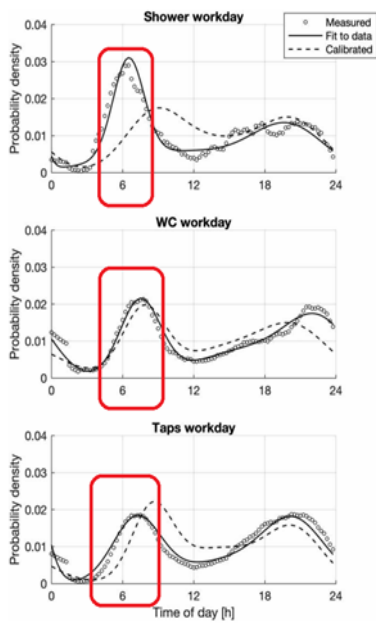


Figure 4 Probable water consumption during the day [10]



Figure 5 Measured hot water flow during the working week [8]

Based on these assumptions, we proposed a daily water consumption model (see Figure 6).

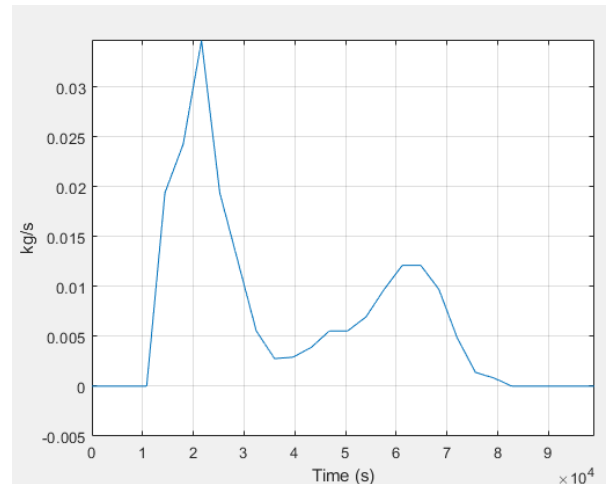


Figure 6 Water consumption model for the working day

#### 4 Wastewater tank construction

We designed the waste water tank as a cylinder with a volume of 21 m<sup>3</sup> and dimensions of 3 m in diameter and height. The spiral-shaped collector is built of DN 32 pipe and will be connected to the interior wall of the tank at its height and perimeter. The working medium of the collector is a 35 % mixture of ethylene glycol and water. The tank's and collector's material is polyethylene, which we have chosen as the building material. The collector has a length of 361 m and a total heat exchange surface area of 45.36 m<sup>2</sup>.



Figure 7 Wastewater tank with collector

The first part of the system is the DHW tank, in which the water temperature ranges from 50 to 60°C. The volume of the tank is kept in equilibrium so that the water input (10°C) to the tank equals the water output

from the tank. The outflow from the tank is 30 % of the total wastewater flow for a given time (Figure 6).

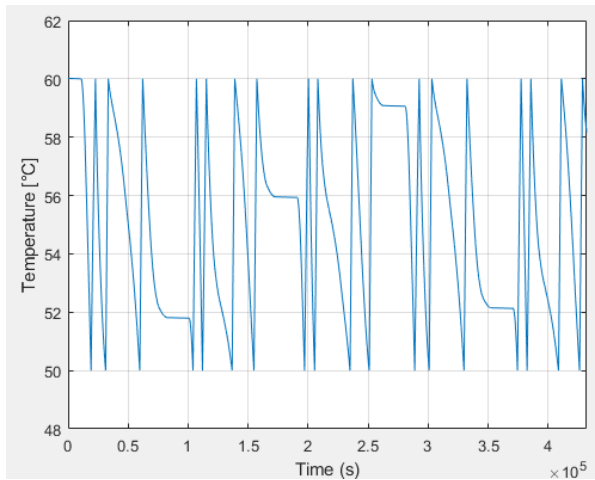


Figure 8 Water temperature in the DHW tank

Another part is the waste water tank. The wastewater supply consists of a mixture of cold (70 %) and hot (30 %) water at the flow rate from the water consumption model for the time. The equation of conservation of energy in a volume of liquid in a tank is:

$$m(C_p - h\alpha)\dot{T} = \phi_{in} - \dot{m}_{in}h + Q \quad (1)$$

Assumptions of the analysis:

- The tank cell is placed at a non-freezing height
- The water in the tank will be no more than 5°C, so heat from the ground will only be transported to the tank and not vice versa.
- The heat transport between the surroundings (ground) will be solved as heating of the semi-infinite solid.
- Heat accumulation in the walls of the tank.

The collector located in the waste water tank will serve as a heat exchanger with ethylene glycol as the working medium. The collector will transport the energy from the wastewater to the working medium, which can be the heat source for the heat pump evaporator. We have set the inlet temperature of the ethylene glycol to -5°C (assumed outlet temperature of the heat pump evaporator).

## 5 Results

The calculation was performed in Matlab software. The analysis was performed for one working week. We assumed that the daily water consumption would be repeated for each day of the week. The calculation was performed for each second of the working week.

In the figure, you can see the maximum collector output concerning the flow rate and temperature of the water in the waste water tank. The performance strongly depends on the amount of water flowing into the tank (see Figure 6). At the beginning of the calculation, the collector shows a power output of more than 4 kW due to an initial volume of 3500 l and a water temperature of 5 °C (the water in the tank has reached thermodynamic equilibrium with the surroundings). Subsequently, we can see the steady-state performance of the collector. The maximum and minimum steady-state collector power were 3113 W and 475 W respectively.

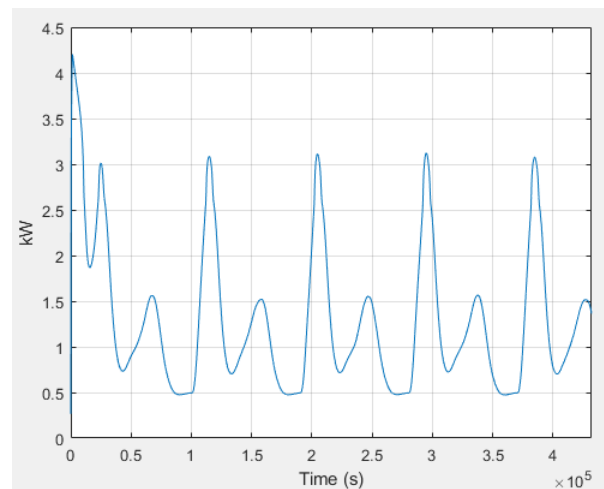


Figure 9 Maximum collector output

The flow rate of the collector was chosen so that the collector can transport the actual amount of energy in the wastewater tank over the course of an hour (see figure).

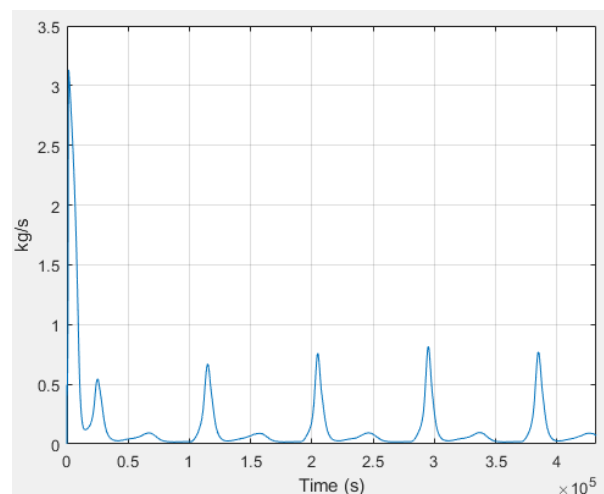


Figure 10 Flow rate of collector

The inlet temperature of ethylene glycol to the collector is -5°C. Depending on the output of the collector, the difference between the inlet and outlet

temperature varies from 1 to 7°C. If the flow through the collector does not stop completely the collector will transport the heat generated by the surroundings of the tank (see figure).

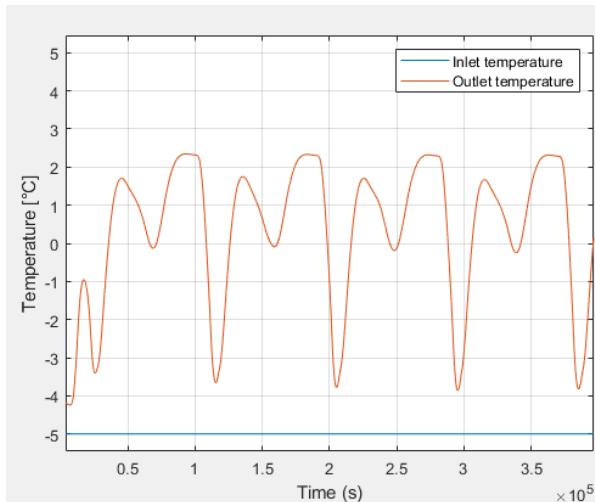


Figure 11 Inlet and outlet temperature of the collector

In the figure, we can see the share of the output of the outdoor unit in the total required output for DHW preparation. The required output for DHW preparation depends on the actual temperature of the water in the DHW tank. As long as the DHW water temperature is not less than 50°C, the system does not produce any power. When the DHW temperature reaches 5°C and the heat from the tank can be transported to the evaporator of the heat pump. The heat pump will then provide the required increase in the energy quality and its transport to the DHW tank.

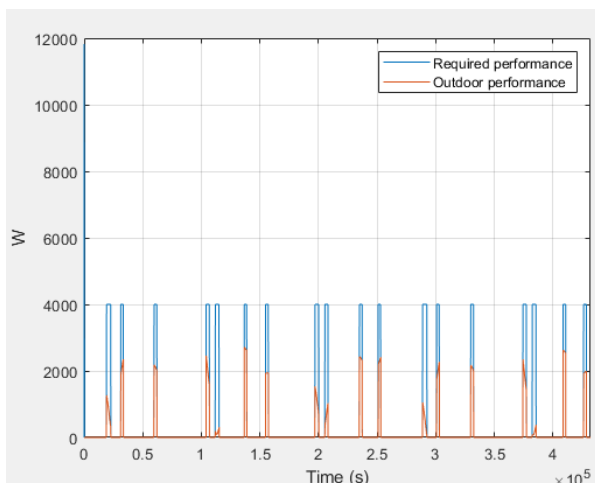


Figure 12 Share of required performance

## Conclusions

If the European Union is to achieve its ambitious environmental targets, it is essential to increase our

efficiency in the use of energy in the home. Wastewater heat recovery has great potential in reducing household energy demand. By placing a collector in the wastewater tank, we can supply more than 50 % of the energy needed to prepare DHW during peak demand periods. In order to accurately determine the energy potential of the wastewater tank, we need to know as accurately as possible the flow and temperature data. No literature or standard has such information so further research is still needed in this area.

## 6 The reference list

- [1] European Commission, Investing in a climate-neutral future for the benefit of our people, 2020.
- [2] ec.europa.eu: EU overachieves 2020 renewable energy target, [Online], Available: [shorturl.at/fgtUZ](https://shorturl.at/fgtUZ) [3 March 2022], 2022.
- [3] The European Parliament and The Council, Directives on the promotion of the use of energy from renewable sources, 2018.
- [4] NAGPAL, H.; SPRIET, J.; MURALI, M.K.; MCNABOLA, A.: Heat Recovery from Wastewater—A Review of Available Resource. *Water*, Vol. 13, No. 9, pp. 1274, 2021.
- [5] CIPOLLA, S.S.; MAGLIONICO, M.: Heat Recovery from Urban Wastewater: Analysis of the Variability of Flow Rate and Temperature, *Energy and Buildings*, Vol. 69, pp. 122-130, 2014.
- [6] CECCONET, D.; RAČEK, J.; CALLEGARI, A.; HLAVÍNEK, P.: Energy Recovery from Wastewater: A Study on Heating and Cooling of a Multipurpose Building with Sewage-Reclaimed Heat Energy, *Sustainability*, Vol. 12, No. 1, pp. 107, 2020.
- [7] ARNELL, M.; LUNDIN, E.; JEPSSON, U.: *Sustainability Analysis for Wastewater Heat Recovery - Literature Review*, Lund University Technical Report, p. 41, 2017.
- [8] KRAFČÍK, M.; PERÁČKOVÁ, J.: What are the cold and hot water flow rates in an apartment building in Bratislava? [Online], Available: [shorturl.at/A3579](https://shorturl.at/A3579) [3 March 2022], 2018
- [9] enviroportal.sk: Specific water consumption per person, [Online], Available: [shorturl.at/bGN67](https://shorturl.at/bGN67) [3 March 2022], 2016

[10] WÄRFF, C; et al.: Modelling Heat Recovery Potential from Household Wastewater. *Water Science & Technology*, Vol. 81, No. 8, pp. 1597–1605, 2020.

### **Acknowledgement**

This publication has been produced with the support of the projects KEGA 021ŽU-4/2021 Conversion of Primary Energy into Heat/Cold Using Thermodynamic Cycles and Compressor Circulation with the Working Substance (refrigerant) CO<sub>2</sub>, KEGA 032ŽU-4/2022—Implementation of Knowledge about Modern Ways of Reducing Environmental Burden in the Energy Use of Solid Fuels and Waste in the Pedagogical Process and VEGA 1/0233/19 Construction modification of the burner for combustion of solid fuels in small heat sources.